High-throughput detection and quantification of phosphatidylcholines and sphingomyelins from single cells by chip-based nanoelectrospray ionisation

Sarah E Hancock[1]†*, Eileen Ding[1], Emma Johansson Beves[2], Todd Mitchell[3,4,5], Nigel Turner[1]†*

[1]Mitochondrial Bioenergetics Laboratory, Department of Pharmacology, School of Medical Sciences, UNSW Sydney, Australia.
[2]Flow Cytometry Unit, Mark Wainwright Analytical Centre, UNSW Sydney, Australia
[3]School of Medicine, University of Wollongong, Wollongong Australia
[4]Illawarra Health and Medical Research Institute, University of Wollongong, Wollongong Australia
[5]Molecular Horizons, University of Wollongong, Wollongong Australia

* corresponding author. Email n.turner@unsw.edu.au & sarah.hancock@unsw.edu.au

† present address: Cellular Bioenergetics Laboratory, Victor Chang Cardiac Research Insititute, Sydney, NSW, Australia.

Abstract

Recent advances in single-cell genomics and transcriptomics technologies have transformed our understanding of cellular heterogeneity in growth, development, ageing and disease. Despite these advances, however, single-cell metabolite profiling (i.e., metabolomics) methods have comparatively lagged behind due to limitations in technology. We have developed a high-throughput method for the detection and quantification of a wide range of phosphatidylcholine (PC) and sphingomyelin (SM) species from single cells that combines fluorescence-assisted cell sorting (FACS) with automated chip-based nanoelectrospray ionisation (nanoESI) and shotgun lipidomics. We show herein that our method is capable of quantifying more than 50 different PC and SM species from single cells and can easily distinguish between cells of different lineages or cells treated with exogenous fatty acids. Moreover, our method can detect more subtle differences in the lipidome between cell lines of the same cancer type. Our approach has the capacity to be run in parallel with other single-cell technologies to deliver near-complete multi-omics data on cells with a similar phenotype and has the capacity to significantly advance our current knowledge on cellular heterogeneity.

Introduction

The recognition that cells of the same lineage (*i.e.,* supposedly identical cells) can present heterogeneous genomic/transcriptomic features has generated great interest in recent years. This work has largely been driven by the development of methods for profiling of single cells, particularly single-cell transcriptomic profiling, and has provided astonishing new insight into the fundamental biological processes of cell heterogeneity and clonal variation in growth, development, and disease[1]. Despite the

37 rapid advances of single-cell genomics and transcriptomics, the development of methods to
38 comprehensively assay metabolites directly from single cells (*i.e.,* single-cell metabolomics) has
39 lagged. This is for several reasons, chief among them being the trace levels of metabolites present within
40 cells (*e.g.,* attomol to low fmol range), the complex array of metabolite present within cells (*e.g.,* 100s
41 to potentially 1000s of different molecules), and an inability to use amplification strategies common in
42 single-cell transcriptomics to augment analyte signal. However, measuring the rapid and dynamic
43 metabolic processes within cells would arguably provide a better phenotypic assessment than that of
44 transcriptomics, which essentially only measures the "potential" of a cell (*i.e.*, not all actively
45 transcribed products are translated downstream).

46 Mass spectrometry (MS) is the current technology of choice for the comprehensive profiling of
47 metabolites from biological tissues due to both its broad specificity in metabolite detection and its
48 sensitivity in detecting very low amounts of analyte from biological samples (*e.g.,* fmol to pmol range).
49 MS is also emerging as a key technology in the detection of analytes from single cells; however, there
50 are some limitations in the sensitivity and/or specificity of currently available technologies. Imaging-
51 based mass spectrometry techniques such as matrix-assisted laser desorption ionisation (MALDI)-MS
52 are perhaps the most developed and utilised single-cell metabolomics techniques in the field to date.
53 MALDI-MS has been used to detect both polar metabolites and lipids from a range of cell types,
54 including algae[2], yeast[3–7], cultured mammalian cells[8], single neurons from pond snails[9,10], plant leaves
55 and/or bulbs[11] and insects[12]. There are, however, several limitations of a MALDI-MS approach to
56 single-cell metabolomics. As its name implies, MALDI requires the application of a matrix to enable
57 ionisation of metabolites, and the type of matrix used can limit the type of metabolite able to be detected.
58 Furthermore, the MALDI laser width is within the range of 5-20 μM (*i.e.,* the diameter of a mammalian
59 cell), placing limitations on the ability of the method to discriminate signal from single cells in close
60 spatial proximity. Nevertheless, improvements in MALDI-MS data processing have enabled the
61 detection of spatially-resolved metabolites from discrete cell populations co-cultured together[13].
62 MALDI spatial resolution has also been improved through the use of either oversampling techniques or
63 transmission mode MALDI sources, which, when combined with post-source ionisation, can improve
64 both imaging resolution and metabolite signal respectively (*e.g.,* 0.6-2 μM)[14,15]. Secondary ion mass
65 spectrometry (SIMS) is another popular imaging-based MS technique used in single-cell metabolomics,
66 owing to its improved spatial resolution over MALDI (*e.g.,* 50-500 nm). However, SIMS suffers from
67 low molecular ionisation alongside extensive fragmentation of target compounds, limiting both its
68 sensitivity and specificity for metabolite identification. Despite these limitations, SIMS has been used
69 for the detection of metabolites from sea hare single neurons[16], as well as the detection of choline
70 fragments arising from membrane lipids in HeLa cells[17,18]. A related technique, laser-ablation
71 electrospray ionisation (LAESI)-MS, provides slightly poorer spatial resolution (*e.g.,* ~30 μM) with a
72 high level of analyte fragmentation making metabolite identification challenging. LAESI has been used

for the detection of several small polar metabolites (*e.g.,* amino acids and sugars) from onion[19,20] and daffodil[19] bulb single cells.

Direction infusion nanoelectrospray ionisation (nanoESI)-based methods are also commonly in use for single-cell metabolite analysis. NanoESI capillaries are an ideal size for directly sampling and infusing the contents of a single cell into the mass spectrometer for detection. This approach has been used to detect a wide array of polar metabolites and lipids from single cells, including plant cells[21,22] and cultured mammalian cells[23–25]. When coupled with light microscopy this technique can provide spatial information on cells and even sample directly from live cells. However, this process is quite laborious and requires the use of micromanipulators for handling and sampling from single cells, thus limiting its high-throughput potential. Some improvements to the throughputness of the technique have been made through the use of a continuous sampling arm that uses dual-bore quartz needles to sample from cells located on a movable stage (i.e, single probe MS)[26–28]. However, the spray duration per cell is limited (~3 min) and precludes the acquisition of tandem mass spectrometry data crucial for metabolite identification. Improvements in spray duration from a single cell have been made by reducing the flow of analyte into the instrument (*i.e.,* picoelectrospray ionisation)[29]. Using this method Wang and colleagues were able to characterise several biomarkers for different breast cancer cell subtypes[29], including membrane lipid species and nucleotides.

In this work we sought to develop an MS-based single-cell lipidomics workflow that is both high throughput and quantitative. To that end, we combined single cell isolation by fluorescence-assisted cell sorting (FACS) with shotgun lipidomics and a chip-based nanoESI ionisation source. This nanoESI source is fully automated and has been used previously for single cell assay using its liquid-extraction surface analysis (LESA) operating mode[30,31]. In this work we operated the instrument in direct infusion mode following FACS of single cells into a 96 well plate format, allowing us to generate stable nanospray from a single cell for more than 30 minutes. We used a semi-targeted shotgun lipidomics approach that could facilitate both improved sensitivity and provide broad specificity in detecting a range of lipid species that may be present amongst different cell types. Using this approach we have been able to detect and quantify more than 50 discrete phosphatidylcholine (PC) and sphingomyelin (SM) species from single cells isolated from different mammalian cell types, and we demonstrate the utility of our method for detecting potentially clinically relevant heterogeneity in prostate cancer cells.

Results

Detection of phosphatidylcholine and sphingomyelin from single cells

We have developed a high throughput, quantitative method for the analysis of PC and SM from single cells by combining FACS with shotgun lipidomics using chip-based nanoESI. All methods are described in detail below (see Method details). Briefly, to develop this method we grew both

107 immortalised myocytes (C2C12) and hepatocarcinoma cells (HepG2) under the same conditions in 75
108 cm^2 culture flasks. At approximately 80-90% confluency cells were trypsinised and counted.
109 Approximately 1-2 million cells of each type were centrifuged (300 *x* g, 5 min) and resuspended in PBS
110 containing 10% foetal calf serum (FCS) and 2 mM EDTA. This process was then repeated to remove
111 all traces of media. Cells were then sorted by FACS directly into a 96 well plate preloaded with
112 methanol spiked with 0.01% butylated hydroxytoluene (BHT) and internal standards (PC 17:0/17:0 and
113 dihydrosphingomyelin, DHSM, 12:0). Plates were sealed and stored at -80ºC until run. Prior to analysis
114 a small amount of methanol:chloroform containing 5 mM ammonium acetate was added to each well
115 to achieve a final ratio of 2:1 v/v. Samples were then directly infused into the mass spectrometer via the
116 chip-based nanoESI source. Shotgun lipidomics were performed by acquiring a precursor scan for *m/z*
117 184 in positive ion mode to identify any PC or SM species present across a mass range of 640 – 850
118 *m/z*. Data from empty wells containing solvent and internal standards were also acquired for background
119 subtraction.

120 We first acquired baseline precursor *m/z* scans from three independent lots of fifty C2C12 or HepG2
121 cells sorted into a single well by FACS. The resulting mass spectra for C2C12 cells are shown in Figure
122 1A. The data demonstrate a typical profile of both PC and SM species normally detected within C2C12
123 cells, with PC 34:1 (760.6 *m/z*) being the most abundant endogenous species present. Importantly, both
124 PC and SM species are being detected at a similar intensity to that seen with cell extracts obtained using
125 a standard extraction protocol before analysis by shotgun lipidomics (*vide infra*). We next infused up
126 to 18 singly sorted C2C12 or HepG2 cells and acquired the same precursor *m/z* 184 scan, with
127 representative spectra from 7 randomly selected single C2C12 cells shown in Figure 1B. Not
128 surprisingly there was a substantial increase in noise within our single-cell spectra; however, both the
129 relative intensity and masses of each species detected closely matches that obtained from the fifty cell
130 samples (Figure 1A). We calculated the signal-to-noise (S/N) for several PC and SM species at differing
131 intensities (shown on Figure 1B) demonstrating that the intensity of many of the detected PC and SM
132 species are well above the background noise present.

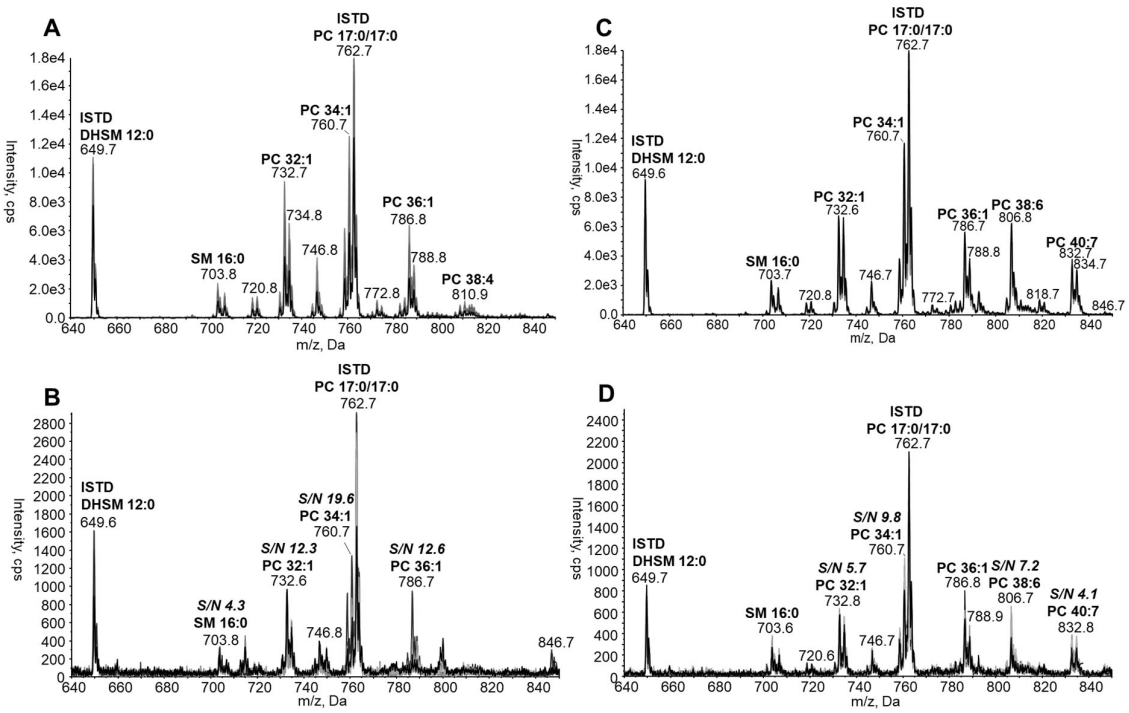

Figure 1: Precursor ion scan of *m/z* 184 obtained from fifty (**A&C**, n=3 biological replicates) and singly isolated (**B&D**, n=7) C2C12 cells obtained by FACS. Cells were grown under normal culture conditions (**A&B**) or cultured overnight in the presence of 50 µM docosahexaenoic acid (DHA, **C&D**). Signal-to-noise (S/N) was calculated using the S-to-N Script in Analyst (v1.6.3, SCIEX, Framingham, MA, USA). Internal standards (ISTD) phosphatidylcholine (PC) 17:0/17:0 & dihydrosphingomyelin (DHSM) 12:0 were added at a concentration of 1 pmol and 1.38 fmol for fifty and single cells respectively.

To confirm that our method was accurately detecting PC and SM species from single cells we performed a second set of experiments in which our C2C12 cells were cultured overnight in the presence of 50 µM docosahexaenoic acid (DHA, 22:6n-3). DHA is an omega-3 (n-3) polyunsaturated fatty acid (PUFA) consisting of 22 carbons and 6 carbon-carbon double bonds, with the first double bond being located at the third carbon from the methyl end of the fatty acid. Vertebrates are unable to synthesise PUFA *de novo* as they lack both the Δ12 and Δ15 desaturases necessary to create either n-3 and omega-6 (n-6) PUFA. Vertebrate cells can elongate and desaturate long-chain PUFA such as linolenic acid (18:3n-3) to form very long-chain PUFA such as DHA, but this conversion is extremely limited within human cells[32]. FCS provides exogenous lipids to cultured cells, but it contains only very low levels of n-3 PUFA[33]. By including DHA within our culture media we can be confident that any detected increase in DHA-containing PC species (*i.e.,* species containing ≥6 carbon-carbon double bonds) can be directly attributed to the experimental conditions and thereby validate our single-cell lipidomics workflow. Overnight culture of C2C12 cells in the presence of DHA indeed produced the expected increase in DHA-containing PC species in both the fifty and single-cell spectra, including noticeable increases in PC 38:6 (806.8 *m/z*), PC 40:7 (832.7 *m/z*), and PC 40:6 (834 *m/z*) (Figure 1C&D respectively). This increase in DHA-containing PC species within the single-cell spectra of DHA-treated cells

156 demonstrates that we are measuring real biological information that is above the noise of the instrument,
157 and together these data establish the validity of our approach for detecting biological variability in the
158 lipids of single cells.

159 The inclusion of internal standards meant that we could perform relative quantitation on both PC and
160 SM species detected from single cells. To achieve this we performed identification of PC and SM
161 species detected from C2C12 and HepG2 single cells (*n*=17-18) with S/N >4 using Lipidview software
162 (v1.3b, SCIEX, Framingham, MA, USA). Lipid species underwent background subtraction before
163 relative quantification from internal standards. All lipid species detected within single C2C12 and
164 HepG2 cells are shown in Figure 2A&B respectively, including those detected under normal culture
165 conditions (CON) and those from media supplemented with DHA. Overall we were able to detect 56
166 distinct PC and SM species from CON and DHA-treated single HepG2 and C2C12 cells. These data
167 not only demonstrated a clear shift in lipid profile in DHA-supplemented cells, but we were also able
168 to observe some inherent heterogeneity in PC and SM species within each of the cell lines and growth
169 conditions. To further explore this heterogeneity we performed t-distributed stochastic neighbour
170 embedding (t-SNE; Figure 3) on our single-cell lipidomics dataset. This analysis showed clear
171 clustering of data from each cell and treatment type, demonstrating that our method can discriminate
172 easily between single cells from both different lineages and culture conditions. Also apparent within
173 the data was some heterogeneity within a given cell line/ fatty acid treatment, which is demonstrated
174 particularly within control HepG2 cells by the spread of the data across the second dimension of the t-
175 SNE plot. Taken together, these data suggest that our single-cell lipidomics method can easily
176 distinguish differences in the lipid profile of single cells isolated from different cell lines and can also
177 detect biological variation driven by the enrichment of exogenous lipid species.

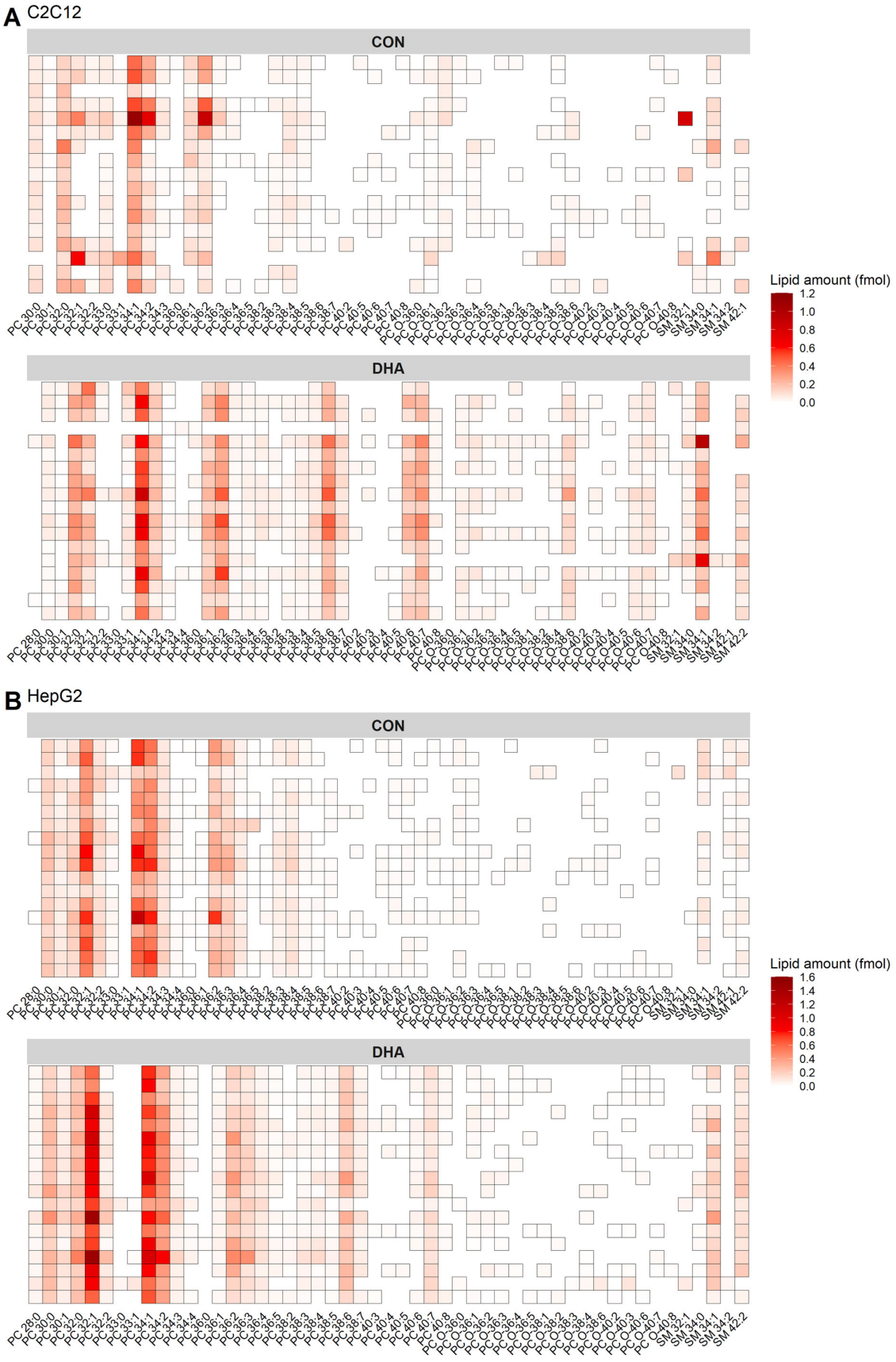
A C2C12
CON
DHA
Lipid amount (fmol)
1.2
1.0
0.8
0.6
0.4
0.2
0.0
B HepG2
CON
DHA
Lipid amount (fmol)
1.6
1.4
1.2
1.0
0.8
0.6
0.4
0.2
0.0

179 **Figure 2:** heatmaps of phosphatidylcholine (PC) and sphingomyelin (SM) species detected in single
180 isolated **A** C2C12 and **B** HepG2cells. Cells were cultured under normal conditions (CON) or after
181 overnight culture with 50 µM docosahexaenoic acid (DHA). Lipids were quantified from internal
182 standards as described under method details and are present as quantified amount (fmol).

183 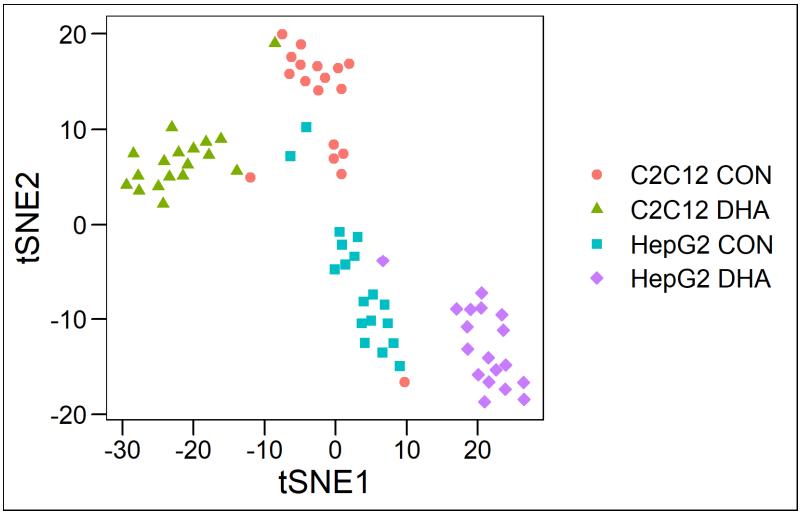

184 **Figure 3:** t-distributed stochastic neighbor embedding (t-SNE) of all single-cell data from both C2C12
185 & HepG2 cells grown in both control (CON) and DHA-supplemented media.

186 **FACS has very little effect on cell PC & SM profile**

187 As FACS is known to change the polar metabolite profile of cells[34] we needed to determine if FACS
188 could also affect the profile of PC and SM present within cells. To that end we compared bulk lipid
189 extracts prepared using the traditional method of lipid extraction from adherent cells (*i.e.,* bulk cell
190 extract) to that of fifty cells isolated by FACS. Full methods for cell extraction and data acquisition are
191 described below (see Method details). Briefly, to obtain bulk cell lipid extracts we grew both C2C12 &
192 HepG2 cells to ~80% confluency in 6 well plates (*i.e.,* ~1 million cells/well, n=3) and extracted each
193 well following overnight exporsure to either control or DHA-supplemented media using a modified
194 MTBE method[35,36]. The organic phase of the bulk cell extract was then diluted approximately 500x with
195 methanol:chloroform (2:1 v/v) containing 5 mM ammonium acetate prior and analysed by shotgun
196 lipidomics. We then compared the relative intensity of both PC and SM species present in the bulk cell
197 extracts with that of fifty cells sorted by FACS from both C2C12 & HepG2 cells grown in either control
198 or DHA-supplemented media (Figure 4). No statistically significant differences in the relative intensity
199 of PC or SM species were detected between bulk cell extracts or fifty-sorted C2C12 cells grown in
200 control media, nor were any differences detected between bulk or fifty-sorted HepG2 cells grown in
201 either control or DHA-containing media. Some small but statistically significant differences were
202 observed between a few relatively minor ether PC species (PC O-38:4, PC O-40:3 and PC O-40:5)
203 between bulk extract and fifty-sorted DHA-supplemented C2C12 cells (Figure 4A); however, these are
204 extremely minor components of the cell membrane. Together these data suggest that FACS has very
205 little impact PC or SM profile, which further supports the validity of our methodological approach.

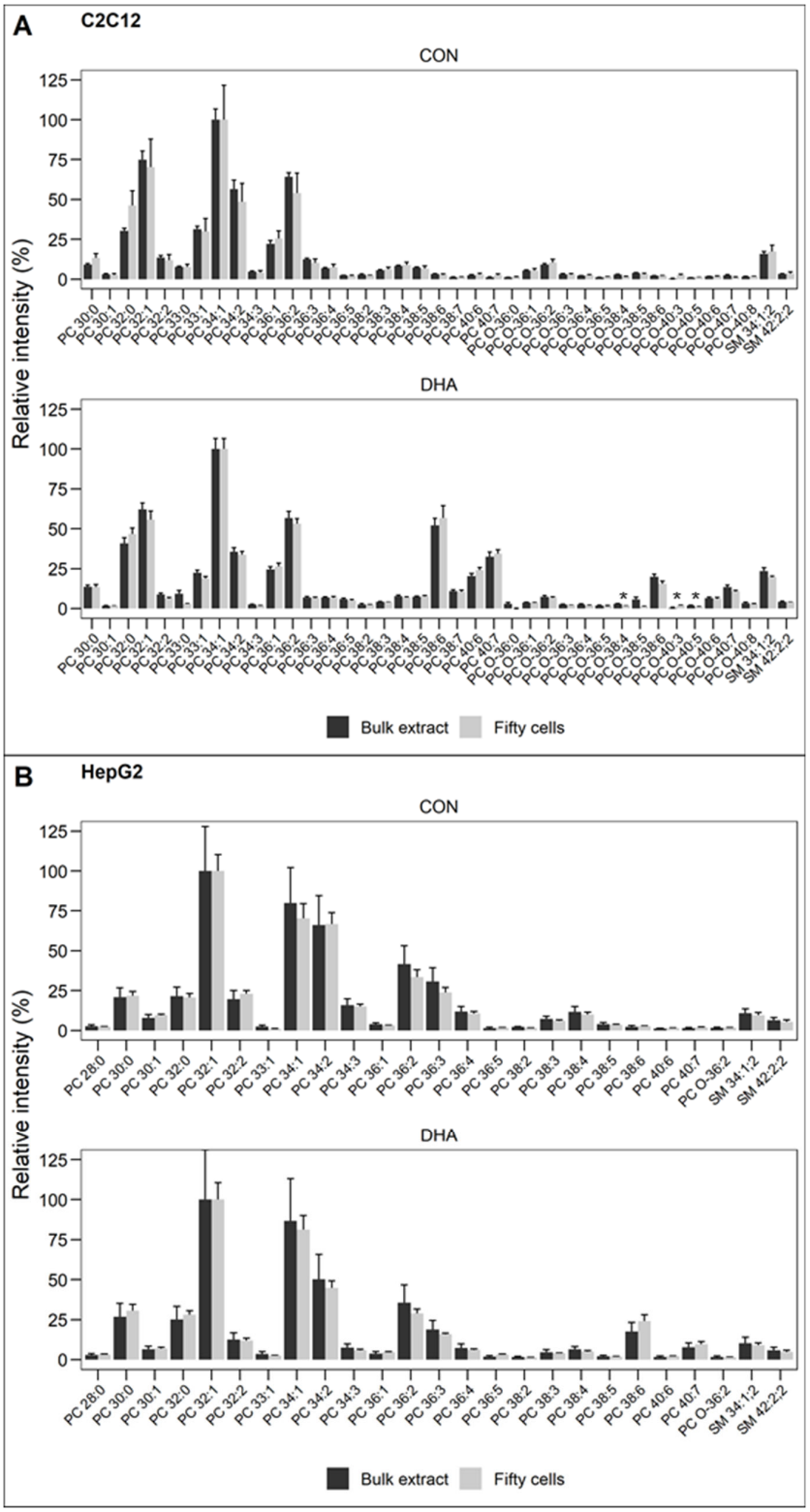

Figure 4: Comparison of PC and SM species detected in either bulk cell extract or fifty cells obtained by FACS for both (**A**) C2C12 cells and (**B**) HepG2 cells treated grown in control (CON) or DHA-supplemented media. Lipids shown are present at >1% relative abundance in either sample, values are mean±SEM (n=3). Welch t-test, * $P < 0.05$. Statistical output from all PC and SM species detected is available in the supplemental material (Table S1).

212 **Single-cell lipidomics can distinguish between different prostate cell lines**

213 In the final part of this work we sought to validate our single-cell lipidomics workflow against an
214 experimental condition with more subtle yet potentially clinically relevant biological heterogeneity. We
215 chose to use prostate cancer as our model for several reasons. First, it is widely reported that PC
216 composition varies between different immortalised prostate cancer cell lines[37–39]. Most recently Young
217 and colleagues reported discrete differences in sum compositional PC species present across six
218 different prostate cancer cell lines[38]. For example, PC 34:1 was reported at ~50% of total PC within the
219 LNCaP prostate cancer cell line, whereas the PC3 cell line purportedly contained ~30% PC 34:1[38].
220 Furthermore, applying single-cell lipidomics techniques to the study of prostate cancer is likely to yield
221 clinically relevant information. Elevated expression of fatty acid synthase (FASN) is common in
222 metastatic, castration-resistant prostate cancer, and higher levels of phospholipids containing saturated
223 and monounsaturated fatty acids are linked with greater metastatic potential in both prostate and other
224 cancer types (reviewed by Butler et al.[40]). Acquired docetaxel resistance in prostate cancer cells can
225 also increase overall PC and SM levels as well as the levels of some specific PC species[39]. For these
226 reasons prostate cancer was chosen as a model for our "proof-of-principle" experiments.

227 To that end we performed shotgun lipidomics on four different prostate cell lines sorted by FACS: three
228 cancerous (DU145, LNCaP & PC3) and a non-tumorigenic immortalised prostate epithelial cell line
229 (PNT1). All cell lines were grown in the same media and were approximately the same passage number.
230 We initially confirmed the heterogeneity reported in the literature PC species between the different
231 prostate cancer cell lines by analysing fifty sorted cells (n=3 per cell line). The resulting PC profile
232 proved to be very similar to that described by Young et al.[38], where PC 34:1 was present at ~48% of
233 total PC in LNCaP cells and ~26% of PC within PC3 cells (Figure 5A). We next performed single-cell
234 lipidomics analysis on the four prostate cell lines (n=18 cells per line) and were able to detect just over
235 50 discrete PC and SM species from single cells (Figure 5B). Not surprisingly, the overwhelming
236 pattern of lipid species abundance in single cells closely mirrored that of the fifty cells data with some
237 heterogeneity being apparent within discrete cells of each line. Finally, we performed t-SNE on our
238 prostate cell single-cell lipidomics dataset, producing the plot shown in Figure 5C. The data broadly
239 clusters into three groups consisting of LNCaP, PC3, and a combination of DU145 and PNT1 cells.
240 This suggests that there is some similarity in lipid profile between DU145 and PNT1 cells that is present
241 even at the single-cell level. Increased heterogeneity appears to be present across the whole prostate
242 single-cell dataset when compared with our previous model of two cell lines of different lineages treated
243 with exogenous fatty acids (Figure 3); however, the data still show relatively tight clustering within the
244 three broad groups of prostate cancer cell lines (Figure 5C). This provides evidence that our single-cell
245 lipidomics workflow is powerful enough to detect more subtle biological variation in cellular
246 heterogeneity such as that found across different cancer cell lines.

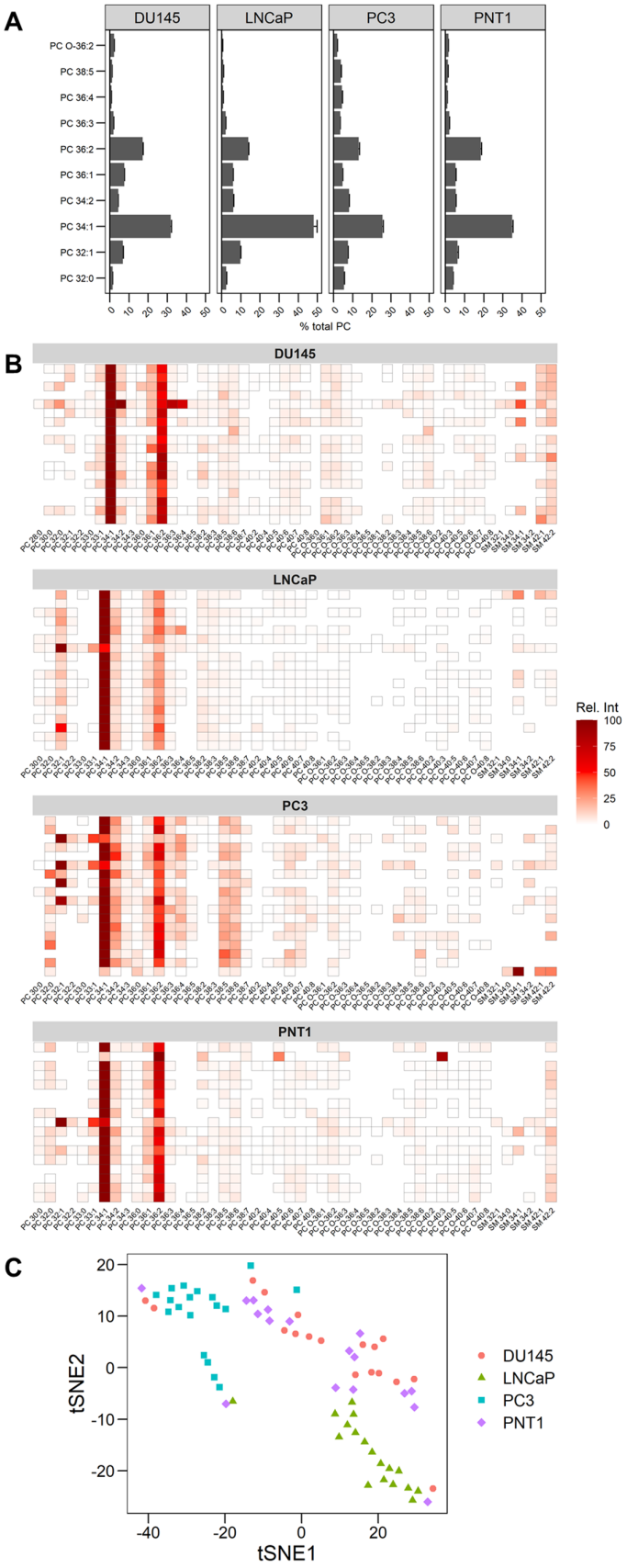
A
DU145
LNCaP
PC3
PNT1
PC O-36:2
PC 38:5
PC 36:4
PC 36:3
PC 36:2
PC 36:1
PC 34:2
PC 34:1
PC 32:1
PC 32:0
% total PC
B
DU145
LNCaP
PC3
PNT1
Rel. Int
100
75
50
25
0
C
tSNE2
tSNE1
DU145
LNCaP
PC3
PNT1

247

248 **Figure 5:** Analysis of PC and SM species from four different prostate cell lines, including cancerous
249 (DU145, PC3 & LNCaP) and non-tumorigenic (PNT1) cells. **A** the ten most abundant PC species
250 detected from the four prostate cell lines. Data acquired from fifty cells obtained by FACS (n=3) and
251 expressed as a percent of total PC (±SEM). **B** PC and SM species detected from single cells across the
252 four prostate cell lines (n=18). Data are expressed as relative intensity within each cell. **C** tSNE of the
253 single-cell data acquired from the four prostate cell lines.

254 ## Discussion

255 In the present study we have described a high-throughput single-cell lipidomics workflow that can
256 detect and quantify a high number of PC and SM species from single cells. To do this we have developed
257 a workflow that combines single-cell FACS with automated chip-based nanoESI and shotgun
258 lipidomics. This workflow utilises a 96-well plate platform for both FACS and mass spectrometry but
259 could be easily adapted to a 384 well plate format to further increase the throughput. We have used this
260 workflow to study single-cell heterogeneity across two different cell lineages and have validated the
261 lipids measured as being true biological measurements by performing experiments designed to
262 manipulate the cell lipidome in a very predictable way (*i.e.,* overnight DHA supplementation, Figures
263 1-3). Using this approach we could detect and quantify more than 50 different PC and SM species within
264 singly-isolated C2C12 and HepG2 cells. We have also applied our method to the study of single-cell
265 lipidome heterogeneity across four different prostate cell lines, including three cancerous (DU145,
266 LNCaP, PC3) and one non-tumorigenic cell line (PNT1). Together these validate the robustness of the
267 method and highlight its potential for detecting clinically relevant parameters.

268 FACS is a common method used for single-cell isolation and is routinely complexed with other single-
269 cell profiling methodologies including transcriptomics. It has been previously reported that FACS can
270 affect the polar metabolome of cells significantly[34]; however, we have determined that it has little to no
271 discernible impact on the PC and SM profile of cells (Figure 4). Other single-cell isolation methods
272 such as microfluidics, magnetic-activated cell sorting, and manual cell picking might also be easily
273 complexed upstream of our single-cell shotgun lipidomics platform in place of FACS if desired.
274 However, use of FACS for single sorting offers the ability to sort cells based on cell surface markers to
275 deliver enhanced information relevant to cell phenotypes. Modern FACS instruments can sort cells by
276 up to 15 or more fluorescently labelled species per cell, which would allow the linking of complex cell
277 phenotypes to their lipidome to provide enhanced detail on phenotype-drive heterogeneity. Moreover,
278 when used in parallel with existing single-cell transcriptomics methods it could provide near-complete
279 multi-omics data acquisition of distinct cell populations sharing phenotypic traits. In turn such data
280 would provide a much more thorough understanding of the role of cellular heterogeneity across a range
281 of fundamental biological and disease-driven research questions and could augment the delivery of
282 personalised medicines for diseases with high levels of inherent lipid heterogeneity (*e.g.,* certain
283 cancers).

284 In this work we chose to apply our method to the study of prostate cancer for two main reasons. Firstly
285 we know that prostate cancer cell lines differ in the abundance of discrete PC species present[37–39] .
286 Furthermore, changes in lipid metabolism have clinical significant in prostate cancer and are highly
287 implicated in its pathogenesis, metastatic potential and resistance to treatment [39,40]. Profiling of PC and
288 SM from singly isolated prostate cancer cell lines revealed both intra- and extra-cell line heterogeneity,
289 and three broad groups of cells were able to be clustered by t-SNE: PC3, LNCaP and a third group of
290 combined DU145 and PNT1 cells (Figure 5C). This is an interesting finding as PNT1 cells are a non-
291 tumorigenic immortalised prostate epithelial line[41], yet show a similar lipidome to CNS metastases-
292 derived DU145 primary prostate adenocarcinoma cells[42]. In terms of metastatic potential, PC3 cells are
293 thought to be the most aggressive, with LNCaP being relatively more quiescent and DU145 somewhere
294 in between[43,44]. The relative abundance of PC species detected within PC3, LNCaP and DU145 prostate
295 cancer cells lines in the present study aligns well with that previously reported[37–39]; however, we could
296 find no publicly available datasets describing the lipidome of PNT1 prostate epithelial cells. Young et
297 al. also described a similar PC profile between DU145 cells and the immortalised BPH-1 prostate
298 epithelial cell line; however, significant differences were observed between phospholipid double-bond
299 positional isomers and the expression of fatty acid desaturase 2 (FADS2) relative to stearoyl-CoA
300 desaturase 1 (SCD1)[38]. This translates to prostate cancer cell lines containing a different fatty acid
301 carbon-carbon double bond profile compared to prostate epithelial cells, but such data cannot be derived
302 using traditional lipidomics profiling by tandem mass spectrometry. We know that extracellular fatty
303 acids heavily influence lipid metabolism in prostate cancer cells[45] and so the lipidome of our DU145
304 and PNT1 cells may simply represent the "default" or baseline lipid profile of prostate cells cultured *in*
305 *vitro* in the absence of any influential biological effect. Future work may focus on complexing our
306 single-cell lipidomics workflow with advanced mass spectrometry-based techniques that can determine
307 more subtle lipid structural information. For example, ozone-induced dissociation could be used to
308 determine carbon-carbon double bond position to enhance the detail of data able to be collected from a
309 single cell [46]. The Paternò-Büchi reaction has also been used to determine carbon-carbon double bond
310 position in single cells, but this reaction requires UV irradiation of the sample through a glass
311 micropipette needle during electrospray and is likely not compatible with our workflow[47]. Such data
312 would likely be of increased clinical relvance in prostate and other cancers, and our method could easily
313 be complexed with techniques such as liquid biopsy to study circulating tumour cells obtained from
314 cancer patients.

315 While developing this workflow we also sought to expand coverage of the single-cell lipidome to
316 include phosphatidylethanolamines (PE), which are typically the second-most abundant class of
317 phospholipid present in mammalian cells. To do this we used a neutral ion loss scan of 141 Da in
318 positive ion mode using settings previously reported[48]. While we could detect numerous PE species in
319 our bulk cell extracts and fifty FACS cell samples, significant contaminant species were detected within

320 our single cell population including ions corresponding with PE 32:0 in both C2C12 and HepG2 cells
321 and PE O-36:5 in HepG2 cells only (Supplemental material, Figure S1). The overall relative intensity
322 of ions detected using our neutral loss scan for PE was also significantly lower than that of PC/SM;
323 leading us to conclude that PE was below the limit of detection for our single-cell method. Charge-
324 switch derivatisation strategies have been successfully used to improve detection in a range of lipid
325 species[49,50], and there is a chemical derivatisation strategy that can impart a fixed positive charge on
326 PE and phosphatidylserine aminophospholipids[51–54]. Future work may target refining such
327 derivatisation strategies to expand lipidome coverage for single cells using our method. Moreover, our
328 approach could be easily adapted to study the polar metabolome, and future work will focus on
329 developing this methodology further. In particular, complexing our method to capillary electrophoresis
330 may yield enhanced coverage and high-throughput assay of the single-cell metabolome[55].

331 In summary, we have developed a high-throughput and quantitative method for the detection of PC and
332 SM lipids from singly isolated cells. Using our method we could quantify more than 50 distinct PC and
333 SM species from single cells of different cell lineages. By using FACS to sort cells our method could
334 be used to provide enhanced data on the relationship between cellular phenotypes and their lipidome,
335 and moreover our approach could be run in parallel with other single-cell methods to deliver near-
336 complete multi-omic assay of cells of similar phenotypes. Our work continues to advance the progress
337 of the development of single-cell metabolomics methods has the potential to improve our knowledge
338 and understanding of cellular heterogeneity.

339 ## Method details

340 ### Cell culture

341 HepG2 and C2C12 cells were obtained from American Type Cell Culture Collection (ATCC; Manassas,
342 Virginia, USA), while prostate cell lines (LNCaP, PC3 DU145, and PNT1) were gifted by Dr Andrew
343 Hoy (University of Sydney Australia). HepG2 and C2C12 were cultured in high-glucose Dulbecco's
344 modified Eagle's medium (DMEM) supplemented with 10% heat-inactivated FCS (Sigma-Aldrich Pty
345 Ltd, Sydney, NSW, Australia) incubated at 37ºC in 5% CO_2. Prostate cancer cell lines were cultured in
346 Roswell Park Memorial Institute (RPMI) medium supplemented with 2 mM L-glutamine and 10% heat-
347 inactivated FCS (ThermoFisher Scientific, Melbourne, VIC, Australia). Medium was changed every
348 three days and cells were passaged at ~80-90% confluency by trypsinisation. Cell lines were regularly
349 screened for mycoplasma infection. Cell number was determined by trypan staining using an automated
350 cell counter (Invitrogen™ Countess II, ThermoFisher Scientific, Melbourne, VIC, Australia).

351 ### DHA supplementation

352 Docosahexaenoic acid (DHA) was obtained from Avanti Polar lipids (Alabaster, AL, USA) and
353 dissolved in 100% ethanol at a concentration of 100 mM. DHA was conjugated to fatty acid-free bovine
354 serum albumin (2% w/v) in media to increase both its solubility and bioavailability [56]. 25 µL of DHA
355 stock or 25 µl of 100% ethanol (CON) was added per 50 mL of normal growth media containing 2%
356 (w/v) of fatty acid-free bovine serum albumin serum (BSA; Sigma-Aldrich Pty Ltd, Sydney, NSW,
357 Australia). Media was sterile filtered by passing it through a 0.2 µM PES filter, and then both CON and
358 DHA-containing media were incubated in a water bath for 2 hours at 55ºC to conjugate DHA to BSA.
359 Conjugated media was then stored at 4ºC until used. Cells were incubated overnight in the presence of
360 CON or DHA-conjugated media prior to harvest.

361 ### Bulk cell lipid extraction

362 All solvents and additives used for lipid extraction were of the highest grade available (either LCMS or
363 HPLC grade) and obtained from ThermoFisher Scientific (Melbourne, VIC, Australia). Bulk cell
364 extracts were prepared from adherent cells grown in 6 well plates. C2C12 cells were seeded at $1x10^5$
365 cells/well and HepG2 at $2x10^5$ cells/well and grown to ~70-80% confluency (~2-3 days). Cells were
366 then treated with CON or DHA-containing media and harvested the following day (final confluency
367 ~80-90%). Media was removed from wells and cells were washed with ice-cold phosphate buffered
368 saline (PBS, pH 7.4). Methanol containing 0.01% BHT (300 µl) was added to each well, and plates
369 were scraped into 2.0 mL eppendorfs. An additional 100 µl of methanol was used to wash each
370 well/scraper and was combined with cell extract. Empty wells were also scraped for background
371 normalisation. To the methanolic cell extracts, 920 µl of methyl tert-butyl ether was added, and samples
372 were vortexed at 1200 rpm for 2-3 hours at room temperature (MixMate ®, Eppendorf South Pacific,

373 Sydney, NSW Australia). Following this, 230 µl of 150 mM ammonium acetate was added and samples
374 were vortexed vigorously for a minimum of 30 seconds. Sample were centrifuged for 5 mins at 2,000 *x*
375 g to induce phase separation, and the upper organic phase was removed to a 2 mL glass vial. This
376 organic phase was then diluted 500-fold in methanol:chloroform (2:1 v/v) containing 5 mM ammonium
377 acetate and stored at -30ºC until analysis. Prior to analysis 40 µl of diluted cell lipid extract was added
378 to a 96 well plate, which was then sealed.

379 **Single cell sorting and lipid extraction**

380 HepG2 and C2C12 cells were grown in 75 cm^2 flasks until ~70-80% confluent before being treated
381 overnight with CON or DHA media. The following day cells (~80-90% confluency) were trypsinised
382 and counted. Prostate cells (LNCaP, DU145, PC3 and PNT1) were grown to ~80-90% confluency
383 before harvest by trypsination followed by cell counting. 1-2 million cells of each line were centrifuged
384 (300 *x* g, 5 min) and resuspended in PBS containing 10% FCS and 2 mM EDTA. This process was then
385 repeated to remove all traces of growth media. Cells were placed on ice and sorted within an hour by
386 FACS (BD FACSAria™ III, BD Biosciences, Sydney, NSW Australia) directly into a 96 well plate
387 preloaded with methanol spiked with 0.01% BHT and internal standards (PC 17:0/17:0 and
388 dihydrosphingomyelin, DHSM, 12:0; Avanti Polar Lipids, Alabaster, AL, USA). Internal standards
389 were added at rate of 1000 fmol per well for fifty cells and 1.38 fmol per single cell. Plates were sealed
390 and stored at -80ºC until analysis. Prior to analysis methanol:chloroform containing 5 mM ammonium
391 acetate was added to each well to achieve a final ratio of 2:1 v/v (final volume 40 µl). Empty wells
392 containing solvent and internal standard only were included for background subtraction.

393 **Mass spectrometry and lipid identification**

394 Nanoelectrospray ionisation (nanoESI) mass spectrometry of lipid extracts was performed using a
395 hybrid triple quadrupole linear ion trap mass spectrometer (QTRAP® 5500, SCIEX, Framingham, MA,
396 USA), equipped with an automated chip-based nanoelectrospray source (TriVersa Nanomate®, Advion
397 Biosciences, NY, USA). PC and SM data were acquired in positive ion mode using a precursor ion scan
398 of *m/z* 184, with spray and acquisition parameters having been described in detail elsewhere [48].
399 Aspiration of 10 µl of sample from each well generated a stable spray time of ≥30 minutes.

400 Lipids were identified from acquired data using Lipidview™ software (v1.2b, SCIEX, Framingham,
401 MA, USA). Processing settings in Lipidview™ were set at a mass tolerance of 0.5 Da, with a minimum
402 intensity of 0.1% and a minimum signal-to-noise ratio of 4. Smoothing and deisotoping of lipid species
403 were enabled. Lipid species were identified from target lists (see supplement material Table S2), and
404 peak area for each detected lipid species was then exported. These data underwent futher processing in
405 R [57], including background subtraction and quantification from internal standards. Lipid nomenclature
406 follows recommendations for the level of molecular detail known [58]; and in the present study we report
407 lipids as class (*e.g.,* PC or SM) followed by the total number of carbons and carbon-carbon double

408 bonds present within the fatty acids separated by a colon (*e.g.,* a PC with 34 carbons and 1 double bond
409 as PC 34:1). At the level of identification available by the technique used in this study some ambiguity
410 exists between isobaric PC species containing either odd-chain or ether-linked fatty acid species, and
411 in the absence of further structural detail we chose to report such species as ether-linked only where
412 overlap exists.

413 **Statistical analysis**

414 Statistical analysis was conducted in R [57], with t-distributed stochastic neighbour embedding (t-SNE)
415 being performed using the Rtsne package [59]. Parameters for t-SNE were set at default values except for
416 perplexity which was set at $\sim N$ ^ (1/2) where N is the number of samples analysed. Comparison between
417 relative intensity of PC and SM species detected from bulk cell extracts and fifty sorted cells was
418 performed using an unpaired t test with Welch's correction, with statistical significance set at $P < 0.05$.

419 ## Acknowledgements

420 This work was supported by a Young Investigator Priority-driven Collaborative Cancer Research Grant
421 awarded to S.E.H. that was funded by Cure Cancer Australia and Can Too! (APP1160909). We thank
422 Dr Andrew Hoy from the University of Sydney for generously gifting us the prostate cell lines used in
423 this work. The authors acknowledge use of the Mass Spectrometry Facility within School of Chemistry
424 at the University of Wollongong.

425 ## References

426 1. Aldridge, S. & Teichmann, S. A. Single cell transcriptomics comes of age. *Nat. Commun.* **11**, 4307
427 (2020).
428 2. Amantonico, A., Urban, P. L., Fagerer, S. R., Balabin, R. M. & Zenobi, R. Single-Cell MALDI-MS
429 as an Analytical Tool for Studying Intrapopulation Metabolic Heterogeneity of Unicellular
430 Organisms. *Anal. Chem.* **82**, 7394–7400 (2010).
431 3. Amantonico, A., Oh, J. Y., Sobek, J., Heinemann, M. & Zenobi, R. Mass Spectrometric Method for
432 Analyzing Metabolites in Yeast with Single Cell Sensitivity. *Angew. Chem. Int. Ed.* **47**, 5382–5385
433 (2008).
434 4. Ibáñez, A. J. *et al.* Mass spectrometry-based metabolomics of single yeast cells. *Proc. Natl. Acad.*
435 *Sci.* **110**, 8790–8794 (2013).
436 5. Urban, P. L. *et al.* High-density micro-arrays for mass spectrometry. *Lab. Chip* **10**, 3206–3209
437 (2010).
438 6. Urban, P. L. *et al.* Carbon-13 labelling strategy for studying the ATP metabolism in individual yeast
439 cells by micro-arrays for mass spectrometry. *Mol. Biosyst.* **7**, 2837–2840 (2011).
440 7. Schmidt, A. M. *et al.* Molecular phenotypic profiling of a Saccharomyces cerevisiae strain at the
441 single-cell level. *Analyst* **139**, 5709–5717 (2014).
442 8. Guillaume-Gentil, O. *et al.* Single-Cell Mass Spectrometry of Metabolites Extracted from Live Cells
443 by Fluidic Force Microscopy. *Anal. Chem.* **89**, 5017–5023 (2017).
444 9. van Veelen, P. A. *et al.* New advanced analytical tools in peptide/protein research: matrix assisted
445 laser desorption mass spectrometry. *J. Controlled Release* **29**, 223–229 (1994).
446 10. Zimmerman, T. A., Rubakhin, S. S., Romanova, E. V., Tucker, K. R. & Sweedler, J. V. MALDI
447 Mass Spectrometric Imaging using the Stretched Sample Method to Reveal Neuropeptide
448 Distributions in Aplysia Nervous Tissue. *Anal. Chem.* **81**, 9402–9409 (2009).

449 11. Gholipour, Y., Nonami, H. & Erra-Balsells, R. Application of pressure probe and UV-MALDI-
450 TOF MS for direct analysis of plant underivatized carbohydrates in subpicoliter single-cell
451 cytoplasm extract. *J. Am. Soc. Mass Spectrom.* **19**, 1841–1848 (2008).
452 12. Neupert, S., Rubakhin, S. S. & Sweedler, J. V. Targeted Single-cell microchemical analysis:
453 MS-based peptidomics of individual paraformaldehyde-fixed and immunolabeled neurons. *Chem.*
454 *Biol.* **19**, 1010–1019 (2012).
455 13. Taylor, M. J., Lukowski, J. K. & Anderton, C. R. Spatially Resolved Mass Spectrometry at the
456 Single Cell: Recent Innovations in Proteomics and Metabolomics. *J. Am. Soc. Mass Spectrom.* **32**,
457 872–894 (2021).
458 14. Niehaus, M., Soltwisch, J., Belov, M. E. & Dreisewerd, K. Transmission-mode MALDI-2 mass
459 spectrometry imaging of cells and tissues at subcellular resolution. *Nat. Methods* **16**, 925–931
460 (2019).
461 15. Bowman, A. P. *et al.* Evaluation of lipid coverage and high spatial resolution MALDI-imaging
462 capabilities of oversampling combined with laser post-ionisation. *Anal. Bioanal. Chem.* (2019)
463 doi:10.1007/s00216-019-02290-3.
464 16. Monroe, E. B., Jurchen, J. C., Lee, J., Rubakhin, S. S. & Sweedler, J. V. Vitamin E Imaging
465 and Localization in the Neuronal Membrane. *J. Am. Chem. Soc.* **127**, 12152–12153 (2005).
466 17. Szakal, C., Narayan, K., Fu, J., Lefman, J. & Subramaniam, S. Compositional Mapping of the
467 Surface and Interior of Mammalian Cells at Submicrometer Resolution. *Anal. Chem.* **83**, 1207–1213
468 (2011).
469 18. Fletcher, J. S. *et al.* A New Dynamic in Mass Spectral Imaging of Single Biological Cells. *Anal.*
470 *Chem.* **80**, 9058–9064 (2008).
471 19. Shrestha, B. & Vertes, A. In Situ Metabolic Profiling of Single Cells by Laser Ablation
472 Electrospray Ionization Mass Spectrometry. *Anal. Chem.* **81**, 8265–8271 (2009).
473 20. Stolee, J. A., Shrestha, B., Mengistu, G. & Vertes, A. Observation of Subcellular Metabolite
474 Gradients in Single Cells by Laser Ablation Electrospray Ionization Mass Spectrometry. *Angew.*
475 *Chem. Int. Ed.* **51**, 10386–10389 (2012).
476 21. Lorenzo Tejedor, M., Mizuno, H., Tsuyama, N., Harada, T. & Masujima, T. In Situ Molecular
477 Analysis of Plant Tissues by Live Single-Cell Mass Spectrometry. *Anal. Chem.* **84**, 5221–5228
478 (2012).
479 22. Yin, R., Prabhakaran, V. & Laskin, J. Quantitative Extraction and Mass Spectrometry Analysis
480 at a Single-Cell Level. *Anal. Chem.* **90**, 7937–7945 (2018).
481 23. Mizuno, H., Tsuyama, N., Harada, T. & Masujima, T. Live single-cell video-mass spectrometry
482 for cellular and subcellular molecular detection and cell classification. *J. Mass Spectrom.* **43**, 1692–
483 1700 (2008).
484 24. Tsuyama, N., Mizuno, H., Tokunaga, E. & Masujima, T. Live Single-Cell Molecular Analysis
485 by Video-Mass Spectrometry. *Anal. Sci.* **24**, 559–561 (2008).
486 25. Date, S., Mizuno, H., Tsuyama, N., Harada, T. & Masujima, T. Direct Drug Metabolism
487 Monitoring in a Live Single Hepatic Cell by Video Mass Spectrometry. *Anal. Sci.* **28**, 201–201
488 (2012).
489 26. Pan, N. *et al.* The Single-Probe: A Miniaturized Multifunctional Device for Single Cell Mass
490 Spectrometry Analysis. *Anal. Chem.* **86**, 9376–9380 (2014).
491 27. Sun, M., Yang, Z. & Wawrik, B. Metabolomic Fingerprints of Individual Algal Cells Using the
492 Single-Probe Mass Spectrometry Technique. *Front. Plant Sci.* **9**, (2018).
493 28. Standke, S. J., Colby, D. H., Bensen, R. C., Burgett, A. W. G. & Yang, Z. Mass Spectrometry
494 Measurement of Single Suspended Cells Using a Combined Cell Manipulation System and a Single-
495 Probe Device. *Anal. Chem.* **91**, 1738–1742 (2019).
496 29. Wang, R. *et al.* Metabolic Discrimination of Breast Cancer Subtypes at the Single-Cell Level
497 by Multiple Microextraction Coupled with Mass Spectrometry. *Anal. Chem.* **91**, 3667–3674 (2019).
498 30. Snowden, S. G. *et al.* Development and Application of High-Throughput Single Cell Lipid
499 Profiling: A Study of SNCA-A53T Human Dopamine Neurons. *iScience* **23**, (2020).
500 31. Ellis, S. R. *et al.* Direct Lipid Profiling of Single Cells from Inkjet Printed Microarrays. *Anal.*
501 *Chem.* **84**, 9679–9683 (2012).
502 32. Burdge, G. C. & Calder, P. C. Conversion of α-linolenic acid to longer-chain polyunsaturated
503 fatty acids in human adults. *Reprod. Nutr. Dev.* **45**, 581–597 (2005).

33. Else, P. L. The highly unnatural fatty acid profile of cells in culture. *Prog. Lipid Res.* **77**, 101017 (2020).
34. Binek, A. *et al.* Flow Cytometry Has a Significant Impact on the Cellular Metabolome. *J. Proteome Res.* **18**, 169–181 (2019).
35. Matyash, V., Liebisch, G., Kurzchalia, T. V., Shevchenko, A. & Schwudke, D. Lipid extraction by methyl-tert-butyl ether for high-throughput lipidomics. *J. Lipid Res.* **49**, 1137–1146 (2008).
36. Abbott, S. K. *et al.* An Improved High-Throughput Lipid Extraction Method for the Analysis of Human Brain. *Lipids* **48**, 307–318 (2013).
37. Sorvina, A. *et al.* Lipid profiles of prostate cancer cells. *Oncotarget* **9**, 35541–35552 (2018).
38. Young, R. S. E. *et al.* Apocryphal FADS2 activity promotes fatty acid diversification in cancer. *Cell Rep.* **34**, (2021).
39. Ingram, L. M., Finnerty, M. C., Mansoura, M., Chou, C.-W. & Cummings, B. S. Identification of lipidomic profiles associated with drug-resistant prostate cancer cells. *Lipids Health Dis.* **20**, 15 (2021).
40. Butler, L. M. *et al.* Lipids and cancer: Emerging roles in pathogenesis, diagnosis and therapeutic intervention. *Adv. Drug Deliv. Rev.* **159**, 245–293 (2020).
41. Cussenot, O. *et al.* Immortalization of human adult normal prostatic epithelial cells by liposomes containing large T-SV40 gene. *J. Urol.* **146**, 881–886 (1991).
42. Stone, K. R., Mickey, D. D., Wunderli, H., Mickey, G. H. & Paulson, D. F. Isolation of a human prostate carcinoma cell line (DU 145). *Int. J. Cancer* **21**, 274–281 (1978).
43. Tai, S. *et al.* PC3 Is a Cell Line Characteristic of Prostatic Small Cell Carcinoma. *The Prostate* **71**, 1668–1679 (2011).
44. Webber, M. M., Bello, D. & Quader, S. Immortalized and tumorigenic adult human prostatic epithelial cell lines: Characteristics and applications part 2. Tumorigenic cell lines. *The Prostate* **30**, 58–64 (1997).
45. Balaban, S. *et al.* Extracellular Fatty Acids Are the Major Contributor to Lipid Synthesis in Prostate Cancer. *Mol. Cancer Res.* **17**, 949–962 (2019).
46. Brown, S. H. J., Mitchell, T. W. & Blanksby, S. J. Analysis of unsaturated lipids by ozone-induced dissociation. *Biochim. Biophys. Acta BBA - Mol. Cell Biol. Lipids* **1811**, 807–817 (2011).
47. Zhu, Y., Wang, W. & Yang, Z. Combining Mass Spectrometry with Paternò–Büchi Reaction to Determine Double-Bond Positions in Lipids at the Single-Cell Level. *Anal. Chem.* (2020) doi:10.1021/acs.analchem.0c02245.
48. Norris, S. E., Friedrich, M. G., Mitchell, T. W., Truscott, R. J. W. & Else, P. L. Human prefrontal cortex phospholipids containing docosahexaenoic acid increase during normal adult aging, whereas those containing arachidonic acid decrease. *Neurobiol. Aging* **36**, 1659–69 (2015).
49. Bollinger, J. G. *et al.* Improved Sensitivity Mass Spectrometric Detection of Eicosanoids by Charge Reversal Derivatization. *Anal. Chem.* **82**, 6790–6796 (2010).
50. Hancock, S. E. *et al.* Mass spectrometry-directed structure elucidation and total synthesis of ultra-long chain (O-acyl)-ω-hydroxy fatty acids. *J. Lipid Res.* **59**, 1510–1518 (2018).
51. Fhaner, C. J., Liu, S., Zhou, X. & Reid, G. E. Functional Group Selective Derivatization and Gas-Phase Fragmentation Reactions of Plasmalogen Glycerophospholipids. *Mass Spectrom.* **2**, (2013).
52. Fhaner, C. J., Liu, S., Ji, H., Simpson, R. J. & Reid, G. E. Comprehensive Lipidome Profiling of Isogenic Primary and Metastatic Colon Adenocarcinoma Cell Lines. *Anal. Chem.* **84**, 8917–8926 (2012).
53. Nie, S. *et al.* Characterization and multiplexed quantification of derivatized aminophospholipids. *Int. J. Mass Spectrom.* **391**, 71–81 (2015).
54. Ryan, E. & Reid, G. E. Chemical Derivatization and Ultrahigh Resolution and Accurate Mass Spectrometry Strategies for "Shotgun" Lipidome Analysis. *Acc. Chem. Res.* **49**, 1596–1604 (2016).
55. Kawai, T. *et al.* Ultrasensitive Single Cell Metabolomics by Capillary Electrophoresis–Mass Spectrometry with a Thin-Walled Tapered Emitter and Large-Volume Dual Sample Preconcentration. *Anal. Chem.* **91**, 10564–10572 (2019).
56. Alsabeeh, N., Chausse, B., Kakimoto, P. A., Kowaltowski, A. J. & Shirihai, O. Cell Culture Models of Fatty Acid Overload: Problems and Solutions. *Biochim. Biophys. Acta* **1863**, 143–151 (2018).

57. R Core Team. *R: A language and environment for statistical computing.* (R Foundation for Statistical Computing).
58. Liebisch, G. *et al.* Shorthand notation for lipid structures derived from mass spectrometry. *J. Lipid Res.* **54**, 1523–1530 (2013).
59. Krijthe, J. J. Rtsne: T-Distributed Stochastic Neighbor Embedding using a Barnes-Hut Implementation. https://github.com/jkrijthe/Rtsne (2015).